Title	Dynamic study of the physical processes in the intrinsic line electromigration of deep-submicron copper and aluminum interconnects(Published)
Author(s)	Tan, Cher Ming; Zhang, Guan; Gan, Zhenghao
Citation	Tan, C. M., Zhang, G., & Gan, Z. (2004). IEEE Transactions on Device and Materials Reliability. IEEE Transactions on Device and Materials Reliability, 4(3), 450-456.
Date	2004
URL	http://hdl.handle.net/10220/6008
Rights	IEEE Transactions on Device and Materials Reliability © 2004 IEEE. Personal use of this material is permitted. However, permission to reprint/republish this material for advertising or promotional purposes or for creating new collective works for resale or redistribution to servers or lists, or to reuse any copyrighted component of this work in other works must be obtained from the IEEE. This material is presented to ensure timely dissemination of scholarly and technical work. Copyright and all rights therein are retained by authors or by other copyright holders. All persons copying this information are expected to adhere to the terms and constraints invoked by each author's copyright. In most cases, these works may not be reposted without the explicit permission of the copyright holder. http://www.ieee.org/portal/site.

Dynamic Study of the Physical Processes in the Intrinsic Line Electromigration of Deep-Submicron Copper and Aluminum Interconnects

Cher Ming Tan, *Senior Member, IEEE*, Guan Zhang, and Zhenghao Gan

Abstract—**Various physical mechanisms are involved in an electromigration (EM) process occurring in metal thin film. These mechanisms are electron-wind force induced migration, thermomigration due to temperature gradient, stressmigration due to stress gradient, and surface migration due to surface tension in the case where free surface is available. In this work, a finite element model combining all the aforementioned massflow processes was developed to study the behaviors of these physical mechanisms and their interactions in an EM process for both Al and Cu interconnects. The simulation results show that the intrinsic EM damage in Al is mainly driven by the electron-wind force, and thus the electron-wind force induced flux divergence is the dominant cause of Al EM failure. On the other hand, the intrinsic EM damage in Cu is driven initially by the thermomigration, and the electron-wind force dominates the EM failure only at a latter stage. This shows that the early stage of void growth in Cu interconnects is more prone to thermomigration than Al.**

Index Terms—**Atom flux divergence, electromigration, electron wind, temperature and stress gradient.**

I. INTRODUCTION

AS THE DIMENSION of metal interconnects is continuously miniaturized to deep submicron level, and new fabrication techniques such as damascene and chemical mechanical polishing as well as new materials are employed, electromigration (EM) continues to be a significant reliability issue in ULSI interconnection. In contrast to a pure diffusion process due only to atom concentration gradient, electromigration in metal thin film is a very complicated diffusion process controlled by various driving forces such as the electron wind, temperature gradient, stress gradient, and surface tension [1]–[3]. These driving forces produce different massflow mechanisms such as electron-wind force-induced migration (EWM), thermomigration (TM), stress migration (SM), and surface migration (SFM). In addition, a healing effect known as the mass

C. M. Tan is with the School of Electrical and Electronics Engineering, Microelectronic Division, Nanyang Technological University, Singapore 639798 (e-mail: ecmtan@ntu.edu.sg).

G. Zhang was with Nanyang Technological University, Singapore. He is now with Integrated Business and Engineering Pte Ltd, Singapore 698527 (e-mail: zgibe@starhub.net.sg).

Z. Gan was with the School of Electrical and Electronics Engineering, Nanyang Technological University. He is now with the School of Materials Engineering, Nanyang Technological University, Singapore 639798 (e-mail: ezhgan@ntu.edu.sg).

backflow due to EM-induced inhomogeneities also plays an important role on the reduction of the EM growth rate [4].

Void formation and growth in metal thin film is a dynamic process where the various massflow mechanisms mentioned above interact with each other to impact the EM behaviors. The interaction between TM and EWM during electromigration damage has long been recognized by means of a thermal loop [5]–[7] as follows. When a void is initiated, the current density is increased around the void due to the reduction in the cross-sectional area of the conductor. Since joule heating is proportional to the square of the current density, the local temperature around the void rises and further temperature gradient exists along the conductor line, which in turn accelerates the void growth.

However, some experimental observations show that there are also other factors affecting EM behaviors. Curry *et al.* [8] reported a mechanism of diffusive cavitations in narrow Al conductor lines under isothermal aging. In this case, voids or open circuits in metal interconnects can occur in the absence of an external current or voltage, and this is attributed to the nonuniform stress distribution in the metal line. Similarly, during EM testing, the thermally induced stress due to the mismatch of the thermal expansion coefficients of materials in an interconnection system can behave in the same way to affect the void growth. As indicated by Korhonen *et al.* [9], void growth provides a source for stress relaxation by dislocation climb or dislocation glide. Therefore, as the void grows, the local temperature difference around the void rises, giving rise to larger thermally induced stress. This stress is then relaxed by void growth, in which electron wind and thermal gradient also play significant roles. Moreover, the presence of the thermally induced stress in metal thin film also leads to a decrease of the threshold product in electromigration, making void damage occur more readily [10].

Arzt and Kraft *et al.* [11], [12] studied the effect of surface tension on EM performance. They proposed that surface tension plays a significant role in the void shape change. This is in good agreement with the theoretical analyses on the morphologies of the stress-induced voids. The void shape appears to be rounded wedgelike if the surface diffusion is sufficient rapid and the EM-induced stress is low in metal thin film. When the opposite is true, the void exhibits narrow cracklike shape [13], [14].

While the above-mentioned massflow mechanisms and their interaction govern the EM process in metal line, the dominant mechanism depends greatly on the metal interconnect material itself. From the usual diffusion path consideration, void failure

in aluminum-based interconnects is dominantly governed by either grain boundary or interfacial diffusion, depending on the grain texture of the thin film; for Cu-based interconnects, interfacial or surface diffusion dominates the void growth. These dominant diffusion paths can be identified easily from the measurement of the activation energy taken in EM testing [15].

On the other hand, few studies are conducted on the identification of the dominant failure mechanisms from a viewpoint of the driving forces. However, such identification is important as it can help to reveal the underlying EM physics in metal interconnect system. As the driving forces are associated with different material properties such as resistivity, thermal conductivity, thermal expansion coefficient, etc., the identification of the dominant driving force allows us to improve the EM performance of metal interconnection system from the perspective of the materials and their integration instead of process or architectural modification of the metal line itself as determined by the dominant mechanism identified based on the diffusion path concept. Examples of the latter modifications are the change in metal layer geometry, deposition and annealing conditions of metal line and its surface treatment.

In the study of the driving forces, most studies are concentrated on the effects due to the electron-wind force and stress gradient, partially due to the much smaller magnitude of the thermomigration as compared to EWM and SM [16]. However, Ru [17] indicated that TM cannot be ignored in electromigration failure because void growth is governed by flux divergence rather than the flux itself. Therefore, in the analysis of electromigration behaviors, TM should also be considered together with other mechanisms as will be done in this work.

Experimentally, it is difficult to identify the dominant driving force during EM testing. Fortunately, the powerful tools of computer simulation make this study possible. From the theoretical models for the various driving forces, the flux divergences due to these forces can be calculated and compared so as to determine the dominant driving force at the different stages of void growth.

Rzepka *et al.* [18] provides a pioneer work to combine all the various driving forces using finite element analysis (FEA) in 1999. However, their study does not consider void growth, and only Al interconnect was studied. Thus, only static study of the electromigration physics was done. In 2001, Dalleau and Weide-Zaage [19] also developed a FEA model for EM simulation from the perspective of driving forces, and dynamic void growth was considered in their model. However, not all the driving forces were included in their model and the interaction as well as dominance of the various driving forces was not studied.

In this simulation work, FEA is employed to study the aforementioned driving forces in the intrinsic EM behavior of deep-submicron Al and Cu interconnects. Through the study of the interaction between the driving forces, the dominant driving force can be determined and explained. The intrinsic EM here refers to the EM process occurring in metal thin film without the effects from the barrier metal and surrounding dielectrics, hence no interface diffusion will be considered. Thus, the intrinsic electromigration studies provide us with a better understanding of the physics of EM in metal and reveal the intrinsic capability of either Al or Cu against EM failure, so that appropriate measures

can be taken to overcome the intrinsic weakness of metal interconnects in EM performance.

II. THEORETICAL BACKGROUND

A void simulation algorithm, including EWM, TM, and SM, has been proposed in detail by Dalleau and Weide-Zaage [19]. However, SFM along void surface was not integrated into their algorithm. In order to reflect the intrinsic EM behaviors more completely, we modify the above algorithm by attaching SFM effect along the free surface of a void.

To study SFM, we first examine the chemical potential of an atom on a free surface. Combining the works on surface migration from Kraft *et al.* [11], [12] and Xia *et al.* [3], there exist three contributions to the chemical potential of an atom on a free surface: 1) free surface energy, μ_0; 2) elastic strain energy stored in the atomic volume; and 3) external current density. Equation (1) gives the chemical potential of an atom on a free surface as follows:

$$\mu = \mu_0 + \Omega(\phi_s - \gamma k) + Z^* e \phi_E \tag{1}$$

where Ω is the atomic volume, $\phi_s = (1/2)\sigma_{ij}\varepsilon_{ij}$ is the elastic strain energy density, γ is the surface tension, κ is the surface curvature, Z^* is the effective valence, and ϕ_E is the electrical potential. σ_{ij} is the stress tensor and ε_{ij} is the strain tensor. The driving force for surface migration is thus derived as follows:

$$\vec{F} = -\nabla\mu = -\Omega(\nabla\phi_s - \gamma\nabla k) + Z^* e \vec{E} \tag{2}$$

where $\vec{E} = -\nabla\phi_E$ is the electric field. According to the Einstein relation, drift velocity of an atom is equal to the product of mobility and driving force. Hence, the flux due to surface migration is given as follows,

$$\vec{J}_{sf} = \frac{\delta_s D_0}{KT} \exp\left(-\frac{E_{sf}}{KT}\right) \left[Z^* e \vec{E} - \Omega\nabla\phi_s + \Omega\gamma\nabla k \right] \tag{3}$$

where δ_s is the effective thickness of the surface diffusion layer, $D_0 \exp(-(E_{sf}/KT))$ is the surface diffusion coefficient, and E_{sf} is the activation energy for surface migration. With (3), the flux divergence due to surface migration can be calculated mathematically.

In the theoretical modeling, diffusion coefficient is an important parameter affecting the mass flux and divergence significantly. Two factors determine the diffusion coefficient, namely the activation energy E_a and pre-exponential factor, D_0. The former is determined by the material and diffusion path, but not related to driving force. Lloyd [15] shows the activation energies along different diffusion paths commonly used in the microelectronics industry. Therefore, for a given test condition and microstructure including grain texture, activation energy is identical for various physical mechanisms due to the various driving forces.

The pre-exponential factor is also dependent only on the material itself with the form of $D_0 = \nu^0\lambda^2$, where ν^0 is Debye frequency dependent only on atom density and speed of sound in the solid, and λ is the jump distance between an atom and a neighboring vacancy [20]. Therefore, for EWM, TM, and SM, the aforementioned two factors for diffusion coefficient are identical. However, it is not true for surface migration because

TABLE I
PHYSICAL PARAMETERS WITH μMKSV UNIT USED IN THE SIMULATION OF AL AND CU INTRINSIC EM

Physical parameter	Symbol	Value		References
		Al	Cu	
Atom concentration	N	$6.03\text{e}10/\mu m^3$	$8.44\text{e}10/\mu m^3$	-
Effective valence charge	Z^*	10	4	[18,21]
Pre-exponential factor for EWM, TM and SM	D_0	$2.3\text{e}8\,\mu m^2/s$	$7.8\text{e}7\,\mu m^2/s$	[22]
Activation energy for EWM, TM and SM	E_a	2.243e-7pJ (1.4eV)	3.525e-7pJ (2.2eV)	[17]
Pre-exponential factor for SFM	D_{sf0}	$1.0\text{e}5\,\mu m^2/s$	$1.4\text{e}4\,\mu m^2/s$	[20]
Activation energy for SFM	E_{sf}	1.602e-7pJ (1eV)	1.25e-7pJ (0.7eV)	[23,17]
Resistivity	ρ_0	$2.65\text{e-}14\,T\Omega.\mu m$	$1.67\text{e-}14\,T\Omega.\mu m$	[21]
Temperature coefficient of resistivity	α	0.0043	0.0039	[24]
Heat of transfer	Q^*	1.221e-8pJ (7.35kJ/mole)	2.773e-8pJ (16.7kJ/mole)	[25]
Poisson ratio	ν	0.35	0.34	[24]
Young's modulus	E	7e4MPa	1.3e5MPa	[24]
Coefficient of thermal expansion	α_l	23.1e-6/K	16.5e-6/K	[24]

it depends both on the diffusion path and driving force. Some of the literature gives the approximate values of the activation energy and pre-exponential factor for surface diffusion [15], [21].

Table I summarizes all the parameter values used in this simulation work, where the activation energy for EWM, TM, and SM is chosen to be 1.4 eV and 2.2 eV for Al and Cu, respectively. This is because: 1) the intrinsic study of EM behaviors does not consider the influence from interface diffusion due to the poor adhesion with the surrounding materials, and 2) the deep-submicron metal layer is of bamboo-like grain texture where grain boundary diffusion is unlikely to occur, making lattice diffusion the most likely diffusion mechanism. Moreover, the stress temperature of 400 °C used in this work also renders lattice diffusion as the dominant diffusion [27], [28].

Fig. 1.   Finite element model used for the study of intrinsic line EM, where a very small void is initialized on the top surface.

III. FINITE ELEMENT MODELING

As we only focus on the underlying physics of the intrinsic EM in deep-submicron metal interconnect in this work, a simple finite element model with dimension of 1 μm (L) $\times$ 0.2 μm (W) $\times$ 0.4 μm (H) is constructed using ANSYS™ [29] as shown in Fig. 1, where a very small void is initialized on the top interface as it is commonly observed experimentally. The local coordinate system is Cartesian system where the x-, y- and z-axes correspond to the direction along the metal length, width, and thickness, respectively. As this study concerns the complex thermal–electrical–mechanical interactions, two couple-field analyses are applied, namely, the thermal–electrical and thermal–mechanical couple-field analyses. In the procedure of generating the finite element model, the element type used in the thermal-electrical analysis is *solid69* with tetrahedral shape constructed by four nodes; for
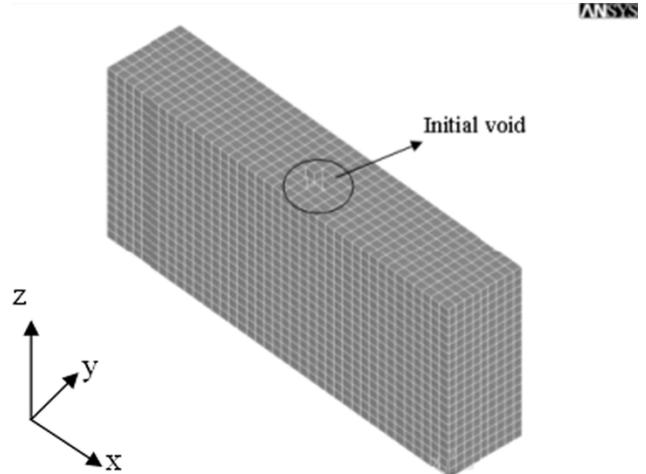
thermal–mechanical analysis, it is replaced by an equivalent structural element type, *solid45*.

In thermal–electrical analysis, the stress current density is 3 MA/cm^2 and the stress temperature is 400 ° C which is applied to the bottom interface of the model [30]. The node temperature distribution obtained in the analysis is then used as the body load in the subsequent thermal–mechanical analysis. In addition, the bottom ($z = 0$) and sidewall interfaces ($y = 0$ or 0.2 μm) are assumed to be constrained as the hardness of the barrier metal is much larger than that of the passivation layer.

Since void growth is a dynamic process, a loop procedure in the simulation is necessary. After each loop, flux divergences due to different driving forces are calculated. Once the atom concentration determined by the total flux divergence reaches the 10% of the initial concentration, the corresponding element is physically deleted, representing the void growth. The time required for a specific void shape is calculated based on the
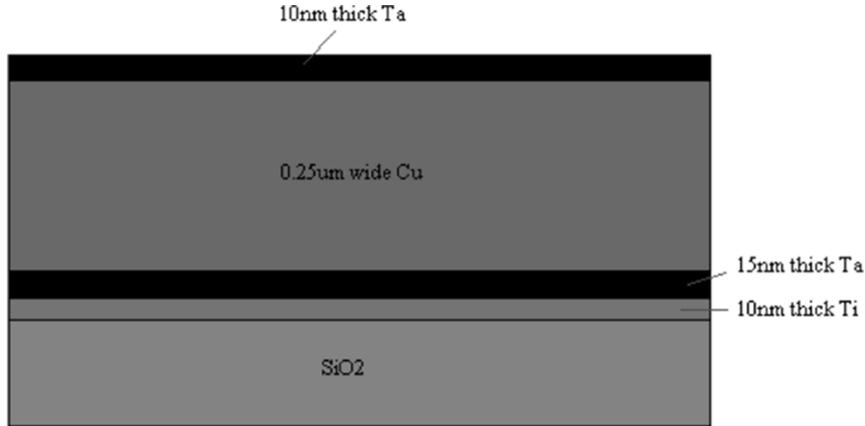
Fig. 2. Schematic cross section of the EM test structure [31].

relationship between the time-to-failure (TTF) and flux divergence proposed by Yu [18], [31], and thus the TTF can be obtained. By analyzing the variation of the flux divergences during void growth, the dynamic behaviors of different driving forces in metal line are revealed.

IV. VERIFICATION OF THE ALGORITHM ON TTF CALCULATION

In order to ensure the validity of this study on the intrinsic EM physics, a verification work is done to examine whether the aforementioned algorithm can correctly calculate the TTF of metal interconnect. An additional purpose of this verification is to investigate whether the resistance change curve obtained from the corresponding finite element model is consistent with the experiment. We chose a known EM test structure proposed by Hu *et al.* [32], which is shown in Fig. 2. Fig. 3 shows the experimental resistance change curves (short-dash lines) for 0.25-μm Cu line extracted from [32].

Since no void nucleation is considered in this simulation work, the TTF cannot be obtained directly from the simulated results. To overcome this problem, the following approach is adopted. The TTF is first obtained for the Cu line with various initial void sizes ranging from 30 to 60 nm, and curve fitting is done to relate the computed TTFs to the initial void sizes. Finally, the extrapolation of the best fitted curve is performed to calculate the TTF of the metal line without initial void. Here, TableCurve 2D™ is used for the curve fitting [33], and the failure criteria is set to be open circuit.

Based on the finite element model representing the test structure shown in Fig. 2, which is an extrinsic case, the simulated ΔR versus time curve for various initial void sizes is shown in Fig. 3 (solid lines), and the corresponding TTFs are summarized in Table II. The test conditions are the same as done by Hu *et al.* [32]. The best fitted curve of TTF versus void size is obtained as follows:

$$y^{-1} = 1.189\,842\,1 + 0.032\,878\,866x \qquad (4)$$

where x is the initial void size and y is the corresponding TTF. This empirical formula not only provides a good fit with coefficient of determination equal to 0.85, it also fulfills the physical
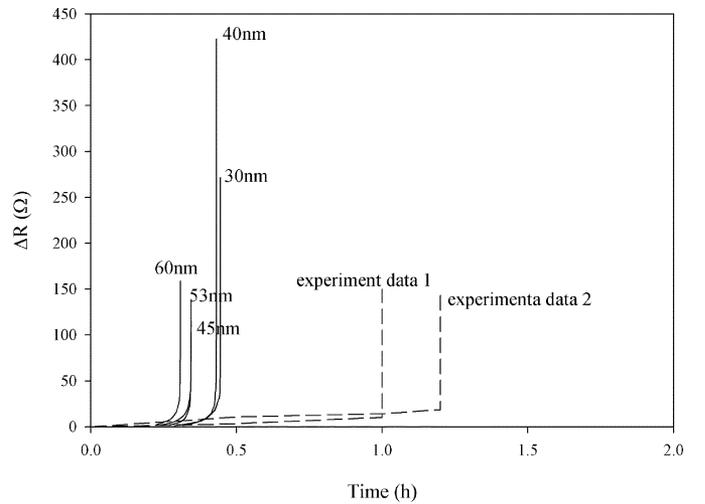

Fig. 3. Resistance change curves from simulation and experiment. (a) Solid lines represent the simulation results in 0.25-μm-wide Cu line with 25 mA/μm^2 at 375 °C, where initial void sizes are 30, 40, 45, 53, and 60 nm, respectively. (b) Short-dash lines are the experimental curves obtained in 0.25-μm-wide Cu line with 25 mA/μm^2 at 375 °C [31].

TABLE II
TTF DATA FROM THE SIMULATION WITH RESPECT TO DIFFERENT INITIAL VOID SIZES

Void size (nm)	TTF from simulation (h)
30	0.4452
40	0.4313
45	0.3445
53	0.3443
60	0.3074

reasoning that TTF increases with decreasing initial void size. By setting $x = 0$, the extrapolated TTF for the specified Cu interconnect without initial void is 0.84 h, which is very close to the experimental TTF value of 1 h shown in Fig. 3 (short-dash lines). Moreover, the ΔR versus time curves from both the simulated and experimental data are also closely resembled. Therefore, the modified algorithm can correctly calculate the TTF in the void simulation, and are suitable for the study of the time-dependent physics in electromigration.
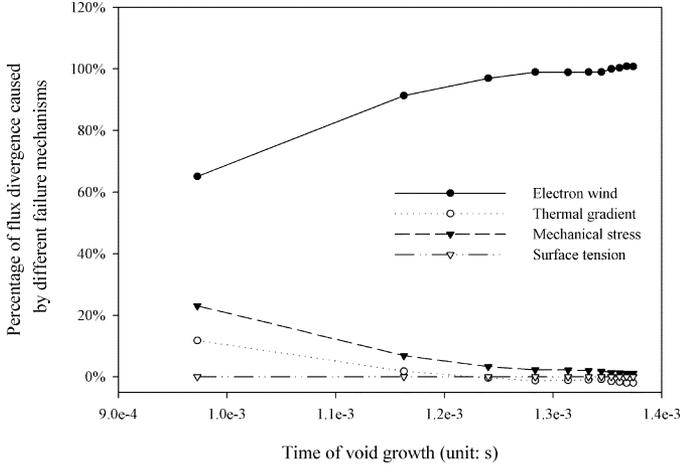
Fig. 4. Change of flux divergences caused by various driving forces during the intrinsic aluminum EM with $j_s = 3$ mA/cm^2 and $T_s = 400\,^\circ$C.

V. ALUMINUM INTRINSIC EM BEHAVIORS

Based on the algorithm described previously, we simulate the void growth in the intrinsic Al electromigration with bamboo grain texture at the stress conditions specified above. The time-dependent variation of the flux divergences due to the various driving forces are plotted in Fig. 4. One can see that, in bamboo Al line, electron wind is the dominant driving force throughout the entire intrinsic EM process. In contrast, other driving forces play insignificant roles, especially in the late stage of the void growth. Moreover, the fact that the TTF is very short indicates that the intrinsic Al metal line is of very low EM resistance, and is fails easily under stress conditions.

The magnitudes of SFM flux and flux divergence are considerably low as compared to those of EWM, TM, and SM. This may be due to the high stress temperature (400 °C) and very narrow linewidth (0.2 μm) used in the simulation. The narrow linewidth reduces the area of void surface, and thus weakens the surface migration. The occurrence of lattice diffusion at high temperature also reduces the proportion of surface-migration-induced massflow in total mass transport.

By analyzing the formulas for calculating various flux divergences, it is easy to understand why the EWM mechanism is dominant in intrinsic Al EM. Substituting the parameter values listed in Table I into the equations derived by Dalleau and Weide-Zaage [18], we have the following expressions governing flux divergences (assuming here the average temperature in Al layer is 400 °C):

$$div(\vec{J}_A) = 8.1 \times 10^{-5}\vec{j} \cdot \nabla T \qquad (5)$$

$$div(\vec{J}_{th}) = -3.196 \times 10^4 \times \nabla T^2 + 4.19 \times 10^{-17}j^2 \qquad (6)$$

$$div(\vec{J}_{st}) = 2.343 \times 10^4 \times \nabla \sigma \cdot \nabla T - 3.182 \times 10^3$$
$$\times \nabla T^2 + 3.667 \times 10^{-17}j^2 \qquad (7)$$

where j is the current density with the range from 3.1×10^{10} to 8.23×10^{10} pA/μm^2, ∇T represents the temperature gradient varying from 0.04 to 3.03 K/μm, and $\nabla \sigma$ is the hydrostatic stress gradient ranging from -0.026 to 0.26 MPa/μm. Note that μMKSV (micrometer-kilogram-second-voltage) unit system is used in this work instead of MKS (meter-kilogram-
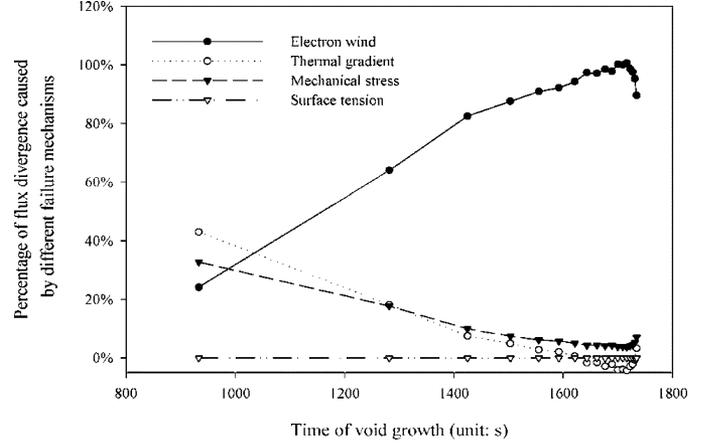

Fig. 5. Change of flux divergences caused by various driving forces during the intrinsic copper EM with $j_s = 3$ mA/cm^2 and $T_s = 400\,^\circ$C.

second) system. From the above equations, it can be clearly seen that there exists a correlation between the flux divergences and the various driving forces as follows:

a) EWM flux divergence $\propto j, \nabla T$;
b) TM flux divergence $\propto -\nabla T^2, j^2$;
c) SM flux divergence $\propto \nabla T \cdot \nabla \sigma, -\nabla T^2, j^2$.

Comparing (5)–(7), and if the temperature gradient is assumed to be constant, the EWM flux divergence is greater than that in TM and SM when the current density is less than 100 mA/cm^2, which is usually the case. By taking the ratio of the EWM flux divergence over either the TM or SM flux divergence, we can also see that the smaller the current density, the larger the proportion of the EWM flux divergence in the total flux divergences, provided the current density is above the threshold current density for EM. We therefore conclude that electron wind is the dominant driving force in the intrinsic Al EM process.

VI. COPPER INTRINSIC EM BEHAVIORS

Fig. 5 shows the variation of the flux divergences due to various driving forces in bamboo Cu line. Unlike the case in Al, the flux divergence due to temperature gradient dominates the Cu void growth at the early stage of the EM process. This implies that the intrinsic Cu is more prone to thermomigration than intrinsic Al. However, their dominances decline with the void growth time, and the proportion of the flux divergence due to EWM increases with time. After a certain time, electron-wind force dominates the void growth until open circuit.

In addition, as shown in Figs. 4 and 5, the TTF of the bamboo Cu line is six orders of magnitude larger than Al under the same stress conditions. This can be explained as follows. Since TTF follows Arrhenius' relationship, it is proportional to the activation energy exponentially. As the activation energies chosen for Al and Cu are 1.4 and 2.2 eV, respectively, in this work, the ratio of the TTF of Cu to Al, under the same stress conditions, is given approximately as follows:

$$r = \exp\left(\frac{1}{K \times 673}(2.2 - 1.4)\right) = 9.91 \times 10^5 \approx 1 \times 10^6. \qquad (8)$$

Therefore, a large difference in TTF is expected theoretically.

Following the analysis used in Al, the equations governing the Cu flux divergences are given as follows:

$$div(J_A) = 1.511 \times 10^{-11} j \cdot \nabla T \tag{9}$$

$$div(J_{th}) = -5.522 \times 10^{-2} \nabla T^2 + 1.84 \times 10^{-23} j^2 \tag{10}$$

$$div(J_{st}) = 1.297 \times 10^{-2} \nabla T \cdot \nabla \sigma - 1.236 \times 10^{-3}$$
$$\times \nabla T^2 + 6.596 \times 10^{-24} j^2 \tag{11}$$

where the range of j is from 3.19×10^{10} to 2.43×10^{11} pA/μm^2, 0.02 to 2.64 K/μm for ∇T, and -0.089 to 0.19 MPa/μm for $\nabla \sigma$. From (9)–(11), the coefficients in the flux divergences for Cu are much smaller as compared with those in Al. This implies that the flux divergences in Cu are much smaller than those in Al, thus Cu has a much larger TTF.

At the initial stage of void growth, the current density in Cu is the same as in Al, but the temperature gradient is much smaller than that in Al. This is because Cu is a better thermal conductor than Al. The smaller temperature gradient in Cu leads to a more uniform thermally induced stress distribution, and thus a smaller stress gradient. Since the TM and SM flux divergences are negatively proportional to the square of the temperature gradient but the reverse is true for the EWM, with much smaller temperature gradient, the thermomigration flux divergence is more dominant than that due to EWM in driving the intrinsic EM damage in Cu as can be seen from (10) and (11). As the void continues to grow, the current density, and hence the temperature gradient, increases rapidly. Therefore, at a later stage, the flux divergence due to electron-wind force will become dominant in the void growth process.

Since interconnect degradation is defined by a failure criterion of resistance change reaching a predetermined value such as 20% or less of the initial resistance, the early dominance of thermomigration in the intrinsic Cu EM calls for greater attention on the thermal properties of Cu and its thermal stability through smart integration of the surrounding materials for the EM improvement in Cu interconnection system.

VII. CONCLUSION

In this work, we modified the existing algorithm by adding the effect of surface migration to study the dynamic natures of the underlying diffusion mechanisms due to various driving force in the intrinsic Al and Cu EM processes. The modified algorithm was verified by computing and comparing the TTF of metal line and the resistance change with the experimental results.

From this simulation work, we conclude that the EM damage in intrinsic Al interconnect is mainly driven by the electron-wind force, and the effects of temperature and stress gradient are found to be insignificant. However, this is not true for the intrinsic Cu EM behaviors, and thermomigration is the dominant driving force in Cu interconnects. Only after a certain time of void growth, the electron-wind force dominates the intrinsic Cu EM failure. This identification of the dominant driving force can help us to improve the EM performance of metal interconnection systems from a materials and integration perspective instead of a process or architectural perspective as derived from the identification of the dominant diffusion path.

REFERENCES

[1] H. B. Huntington, "Effect of driving forces on atom motion," *Thin Solid Films*, vol. 25, no. 2, pp. 265–280, Feb. 1975.

[2] P. G. Shewmon, *Diffusion in Solids*, 2nd ed. Warrendale, PA: Minerals, Metals and Materials Soc., 1989, pp. 30–30.

[3] L. Xia, A. F. Bower, Z. Suo, and C. F. Shih, "A finite element analysis of the motion and evolution of voids due to strain and electromigration induced surface diffusion," *J. Mech. Phys. Solids*, vol. 45, no. 9, pp. 1473–1493, Sept. 1997.

[4] I. A. Blech, "Diffusion back flows during electromigration," *Acta Mater.*, vol. 46, no. 11, pp. 3717–3723, Jul. 1998.

[5] R. A. Sigsbee, "Electromigration and metallization lifetimes," *J. Appl. Phys.*, vol. 44, no. 6, pp. 2533–2540, June 1973.

[6] K. Nikawa, "Monte Carlo calculations based on the generalized electromigration failure model," in *Proc. IEEE 19th Int. Reliab. Phys. Symp.*, 1981, pp. 175–181.

[7] A. P. Schwarzenberger, C. A. Ross, J. E. Evetts, and A. L. Greer, "Electromigration in the presence of a temperature gradient: Experimental study and modeling," *J. Electron. Mater.*, vol. 17, no. 5, pp. 473–478, Sept. 1988.

[8] J. Curry, G. Fitzgibbon, Y. Guan, R. Muollo, G. Nelson, and A. Thomas, "New failure mechanisms in sputtered aluminum-silicon films," in *Proc. IEEE 22nd Int. Reliab. Phys. Symp.*, 1984, pp. 6–8.

[9] M. A. Korhonen, C. A. Paszkiet, and C.-Y. Li, "Mechanisms of thermal stress relaxation and stress-induced voiding in narrow aluminum-based metallization," *J. Appl. Phys.*, vol. 69, no. 12, pp. 8083–8091, June 1991.

[10] J. R. Lloyd, "Electromigration and mechanical stress," *Microelectron. Eng.*, vol. 49, no. 1–2, pp. 51–64, Nov. 1999.

[11] E. Arzt, O. Kraft, W. D. Nix, and J. E. Sanchez Jr, "Electromigration failure by shape change of voids in bamboo lines," *J. Appl. Phys.*, vol. 76, no. 3, pp. 1563–1571, Aug. 1994.

[12] O. Kraft and E. Arzt, "Electromigration mechanisms in conductor lines: Void shape changes and slit-like failure," *Acta Mater.*, vol. 45, no. 4, pp. 1599–1611, Apr. 1997.

[13] T. J. Chuang, K. I. Kagawa, J. R. Rice, and L. B. Sills, "Non-equilibrium models for diffusive cavitation of grain interfaces," *Acta Metallurgica*, vol. 27, no. 3, pp. 265–284, Mar. 1979.

[14] L. Martinez and W. D. Mix, "Numerical study of cavity growth controlled by coupled surface and grain boundary diffusion," *Metallurgical Transactions A (Physical Metallurgy and Materials Science)*, vol. 13A, no. 3, pp. 427–437, Mar. 1982.

[15] J. R. Lloyd, J. Clemens, and R. Snede, "Copper metallization reliability," *Microelectron. Reliabil.*, vol. 39, no. 11, pp. 1595–1602, Nov. 1999.

[16] A. Scorzoni, B. Neri, C. Caprile, and F. Fantini, "Electromigration in thin-film interconnection lines: Models, methods and results," *Mater. Sci. Rep.*, vol. 7, no. 4–5, pp. 143–220, Dec. 1991.

[17] C. Q. Ru, "Thermomigration as a driving force for instability of electromigration induced mass transport in interconnect lines," *J. Mater. Sci.*, vol. 35, no. 22, pp. 5575–5579, Nov. 2000.

[18] S. Rzepka, E. Meusel, M. A. Korhonen, and C. Y. Li, "3-D finite element simulator for migration effects due to various driving forces in interconnect lines," in *Proc. 5th Int. Workshop in Stress Induced Phenomena in Metallization*, 1999, pp. 150–161.

[19] D. Dalleau and K. Weide-Zaage, "Three-dimensional voids simulation in chip metallization structures: A contribution to reliability evaluation," *Microelectron. Reliabil.*, vol. 41, no. 9–10, pp. 1625–1630, Sept.–Oct. 2001.

[20] K. N. Tu, "Interdiffusion in thin films," *Annu. Rev. Mater. Sci.*, vol. 15, pp. 147–176, 1985.

[21] V. P. Zhdanov, *Elementary Physicochemical Processes on Solid Surfaces*. New York: Plenum Press, 1991, pp. 52–52.

[22] S. P. Murarka, I. V. Verner, and R. J. Gutmann, *Copper-Fundamental Mechanisms for Microelectronic Applications*. New York: Wiley, 2000.

[23] W. D. Callister Jr, *Materials Science and Engineering: An Introduction*. New York: Wiley, 2003, pp. 101–101.

[24] R. Stumpf and M. Scheffler, "Ab initio calculation of energies and self-diffusion on flat and stepped surface of Al and their implications on crystal growth," *Phys. Rev. B (Condensed Matter)*, vol. 53, no. 8, pp. 4958–4973, Feb. 1996.

[25] J. F. Shackelford and W. Alexander, *CRC Materials Science and Engineering Handbook*, 3rd ed. Boca Raton, FL: CRC Press, 2001.

[26] R. W. Cahn and P. Haasen, *Physical Metallurgy*, 4th ed. Amsterdam, NY, The Netherlands, 1996.

[27] J. R. Lloyd and R. H. Koch, "Electromigration-induced vacancy behavior in unpassivated thin films," *J. Appl. Phys.*, vol. 71, no. 7, pp. 3231–3233, Apr. 1992.

[28] A. Gladkikh, Y. Iereah, M. Karpovski, A. Palevski, and Y. S. Kaganovski, "Activation energy of electromigration in copper thin film conductor lines," in *Mater. Res. Soc. Symp. Proc.*, vol. 427, 1996, pp. 121–126.

[29] "ANSYS Release 5.6," ANSYS Inc., Canonsburg, PA, 1999.

[30] P. F. Tang, "Simulation and computer models for electromigration," in *Electromigration and Electronic Device Degradation*, A. Christou, Ed. New York: Wiley, 1994, pp. 40–40.

[31] X. Yu, "Untersuchungen zum Einfluß von mechanischem Stress auf die Migration in Metallisierungsstrukturen integrierter Schaltungen," Ph.D. dissertation, Univ. of Hannover, Hannover, Germany, 2000.

[32] C. K. Hu, K. Y. Lee, L. Gignac, and R. Carruthers, "Electromigration in 0.25 μm wide Cu line on W," *Thin Solid Films*, vol. 308–309, no. 1-4, pp. 443–447, Oct. 1997.

[33] "TableCurve 2D v5 for Windows," AISN Software Inc., Mapleton, OR, 2000.

Guan Zhang received the B.Eng. degree in measurement and instrument engineering from Xidian University, Xi'an, China, in 1994, and the M.Eng. degree in electrical and electronic engineering from Nanyang Technological University, Singapore, in 2001.

From 1994 to 1998, he was with Shougang NEC Microelectronics Company Ltd., Beijing, China, as a Senior Equipment Engineer in photolithography process. From 2001, he joined the School of Electrical and Electronic Engineering, Nanyang Technological University as a Research Associate. In May 2004, he joined Integrated Business and Engineering Pte Ltd. as a Senior Research Engineer, mainly focusing on the thermal management of power semiconductor device and reliability and maintainability analysis. His research areas also include electromigration reliability physics of ULSI metal interconnection, finite element analysis of device failure, and reliability data analysis in accelerated lifetime test.

Cher Ming Tan (M'84–SM'00) received the B.Eng. (Hons.) degree from the National University of Singapore in 1984 and the M.A.Sc. and Ph.D. degrees from the University of Toronto, Toronto, ON, Canada, in 1988 and 1992, respectively, all in electrical engineering.

From 1992 to 1996, he was with LiteOn Power Semiconductor Corporation, Taiwan, R.O.C., as a Quality and Reliability Manager and an Engineering Consultant. In 1996, he joined Chartered Semiconductor Manufacturing, Ltd., Singapore, as a Quality and Reliability Section Manager. In 1997, he joined the School of Electrical and Electronic Engineering, Nanyang Technological University as a Lecturer on IC reliability failure analysis. His current research areas include reliability data analysis, electromigration reliability physics and test methodology, silicon wafer defect study, quality engineering, and silicon-on-insulator structure fabrication technology.

Dr. Tan is currently listed in *Who's Who in Science and Engineering* as well as *Who's Who in the World*.

Zhenghao Gan received the B.Eng. and M.Eng. degrees in materials science and engineering from Zhejiang University, Hangzhou, China, in 1995 and 1997, respectively, and the Ph.D. degree in mechanical engineering from Nanyang Technological University, Singapore, in 2002.

He is currently a Research Fellow with the School of Materials Engineering, Nanyang Technological University. His research interests include interconnect reliability and failure analysis of nanoelectronic materials and devices, lead-free solder joints, thin films, and finite element analysis (FEA).